International Journal of Pharmaceutics 584 (2020) 119430

Contents lists available at ScienceDirect

International Journal of Pharmaceutics

journal homepage: www.elsevier.com/locate/ijpharm

Formulation design for inkjet-based 3D printed tablets

Koyel Sen[a], Arushi Manchanda[a], Tanu Mehta[a], Anson W.K. Ma[b,c], Bodhisattwa Chaudhuri[a,b,c,*]

[a] Department of Pharmaceutical Sciences, University of Connecticut, United States
[b] Department of Chemical and Biomolecular Engineering, University of Connecticut, United States
[c] Institute of Material Sciences, University of Connecticut, United States

ARTICLE INFO

Keywords:
3D printing
Binder-jet 3D printing
Drug loading efficiency
Additive manufacturing

ABSTRACT

The drug loading efficiency was evaluated using a binder-jet 3D printing process by incorporating an active pharmaceutical ingredient (API) in ink, and quantifying the printability property of ink solutions. A dimensionless parameter Ohnesorge was calculated to understand the printability property of the ink solutions. A pre-formulation study was also carried out for the raw materials and printed tablets using thermal analysis and compendial tests. The compendial characterization of the printed tablets was evaluated with respect to weight variation, hardness, disintegration, and size; Amitriptyline Hydrochloride was considered as the model API in this study. Four concentrations of the API ink solutions (5, 10, 20, 40 mg/mL) were used to print four printed tablet batches using the same tablet design file. The excipient mixture used in the study was kept the same and consists of Lactose monohydrate, Polyvinyl pyrrolidone K30, and Di-Calcium phosphate Anhydrate. The minimum drug loading achieved was 30 μg with a minimal variation (RSD) of < 0.26%. The distribution of the API on the tablet surface and throughout the printed tablets were observed using SEM-EDS. In contrast, the micro-CT images of the printed tablets indicated the porous surface structure of the tablets. The immediate release properties of the printed tablets were determined using a dissolution study in a modified USP apparatus II.

1. Introduction

The interest in 3D printing applications has been extended to the pharmaceutical industry very recently due to the additional aptitude of the printing process, such as complex drug release, complex drug product geometries, personalization, and unique drug loading efficiency (Khaled et al., 2014; Rowe et al., 2000). It has been widely believed that the future of medicine is personalization to the point of designing medicine, such as tablets for individual patients (Sandler et al., 2011). Tablets, by far the commonly used pharmaceutical dosage form, have been the most studied area due to its ease of administration, patient compliance, and low cost of manufacturing (Sastry et al., 2000; Jivraj et al., 2000).

Unfortunately, the current technologies available for conventional tablet manufacturing processes require several unit operations, including mixing, milling, granulation, drying, compression, etc. (Unit Processes in Pharmacy, 2013). Moreover, it also entails knowledgeable personnel and several expensive instruments which require an immense investment of time and money, resulting in a burdensome amount cost for consumers of oral dosage formulations available in the market (Scoutaris et al., 2011). However, after all these investments, there still exists a shortage of advanced technologies to manufacture personalized medicine with the currently available settings (Skowyra et al., 2015; Tutton, 2012).

3D printing can circumvent this gap by providing the ability to design personalized medicines precisely. Previous studies by other researchers have shown that personalization of medicine can be achieved by 3D printing (Stability of Drugs and Dosage Forms, 2002). Khaled et al. (2014) fabricated a control-released pharmaceutical bi-layer tablet using an extrusion-based Desktop 3D printer. Wang et al. (2016) successfully used the stereolithographic 3D printing process to develop modified release oral dosage forms (Tutton, 2012). Whereas Okwuosa et al. (2016) developed an immediate release oral dosage form using a lower temperature fusion deposition modeling 3D printing process (Okwuosa et al., 2016). The focus of this study was to evaluate pharmaceutical tablet and dosage form fabrication using an inkjet-based 3D printing process.

Binder jet 3D printing is an inkjet-based 3D printing process in which the ink drops are jetted out of a nozzle and are deposited on top of a powder surface in a layer-by-layer fashion to fabricate a three-dimensional object, in this case a tablet. To manufacture a pharmaceutical tablet dosage form using an inkjet-based 3D printing process,

* Corresponding author at: Department of Pharmaceutical Sciences, University of Connecticut, Storrs, CT, USA.
E-mail address: bodhi.chaudhuri@uconn.edu (B. Chaudhuri).

https://doi.org/10.1016/j.ijpharm.2020.119430
Received 5 March 2020; Received in revised form 4 May 2020; Accepted 9 May 2020
0378-5173/

an excipient mixture and an ink/binder were loaded onto the printer as feedstock materials.

The advancement of 3D printing applications in the pharmaceutical industry is at its nascent stage and only recently, after the marketing of the one and only FDA approved 3D printed tablet by Aprecia Pharmaceuticals in 2015, has it gained attention (SPRITAM, xxxx). There are currently several research groups working with different 3D printing processes to evaluate their applicability in manufacturing the pharmaceutical dosage form (Genina et al., 2013). To date, the only printing process that came into the FDA's approval limelight was Binder jetting; used when Aprecia Pharmaceutical marketed their first 3D printed tablet, 'Spritam.' The first FDA approved 3D printed tablet Spritam is a levetiracetam tablet with orodispersible properties and lower mechanical strength. Unlike the conventional tablet manufacturing, the inkjet-based 3D printing process lacks a compression step, thus providing a porous, fragile and fast dissolving tablet structure at the end of a printing cycle. Spritam was manufactured by adding water as a liquid binder to a powder mixture of active pharmaceutical ingredient (API) and excipients using a binder jet 3D printing process (Gala et al., 2019).

The binder jet 3D printer requires both powder and binder liquid feedstock materials. The powder forms the bulk of the printed structures as the liquid feedstock binds the powder together. Much like any day to day printing process, an image file needs to be developed and sent to the printer prior to the printing process. The printer used for the experiment consists of a tote-shaped hopper to store the excipient mixture (Fig. 1), reservoirs to load the ink/binder, and thermal printheads to jet out the ink in small droplets. The printing process occurs on the build platform, as shown in Fig. 1. During the printing, the printer discharges a specific amount of the excipient/powder mixture from the hopper, and a roller spreads the powder in a thin layer like a sheet onto the build platform. Afterward, the printheads collect the ink for the reservoirs and precisely spray the powder surface on top, followed by the design of the image file. Thus, developing 3D printed tablets in a layer-by-layer approach. Once a printing cycle is over, the printed tablets are heated at 40 °C to consolidate the samples for further characterization tests.

The innovation of this study rests upon the idea of evaluating the drug loading efficiency of the inkjet-based 3D printing process by including the API in ink instead of adding it to the powder mixture. Firstly, for engineering the drug release profile, it is much easier to vary the concentration of one or multiple drugs with the printed samples ("printlets") through ink fluids, in the same way that different colors are used for graphics printing, instead of varying the composition of the powder added in successive layers (Alomari et al., 2015). Secondly, adding the API through the ink does not require blending the API with the excipients, reducing the amount of API required per experiment, which is more desirable from the material usage and reuse perspective. However, the inclusion of the API also modifies the ink fluid properties which may, in turn, hinder the jetting process (Guo et al., 2017). Thus, if the API is jetted, the dose level must be precisely controlled (Alomari et al., 2015).

In this paper, we have evaluated the drug loading efficiency of the binder-jet 3D printing process along with the pre-formulation study of the binder-jet 3D printed tablets. Amitriptyline HCl was used as a model drug because of its higher stability and aqueous solubility in the ink solution. Four different concentrations (5, 10, 20, 40 mg/mL) of API inks and one excipient mixture were selected for the study. The API inks were characterized and evaluated with regards to their printability/jettability property, whereas the excipient mixture and printed tablets were evaluated through pre-formulation characterization. Moreover, the printed tablets were also characterized with respect to their structure, hardness, content uniformity, and *in vitro* release patterns.

2. Materials & methods

2.1. Materials

Amitriptyline Hydrochloride (AMT) was selected as the model drug or active pharmaceutical ingredient (API) and was obtained from Teva Pharmaceuticals (Parsippany, NJ, USA). One of the excipients Lactose Monohydrate was attained from DFE Pharma (Taranaki, New Zealand). The other excipients, Di-Calcium Phosphate Anhydrate and PVP K30 (Polyvinyl Pyrrolidone), were obtained from Innophos Nutrition (Illinois, Chicago, USA), and JRS Pharma (New York, USA), respectively.

Preparation of ink/binder solution-The API in the printed tablets was delivered via the ink solution used in printing. Four types (different drug concentrations) of ink solution were prepared by dissolving AMT in deionized- distilled water (with resistance of 18.2Mohm) at varying concentrations of 5, 10, 20 and 40 (mg/mL). All solutions were degassed overnight and filtered under vacuum through 0.22 μm hydrophilic 13 mm diameter polyvinylidene difluoride (PVDF) filter (Millipore, Fisher Scientific, Pittsburgh, PA) prior to loading into the ink reservoirs. The ink solution was sealed with parafilm and covered by alumina foil during sonication and transferred to minimize solvent loss and drug degradation. The ink preparation protocol was kept standard for all of the inks.

Preparation of the excipient mixture-The excipient mixture was prepared in an aluminum (Al) V blender and rotated at 29 RPM for 18 min (Mukherjee et al., 2016). The mixture consists of three pharmaceutical excipients, namely Lactose Monohydrate, PVP K30, and Di-

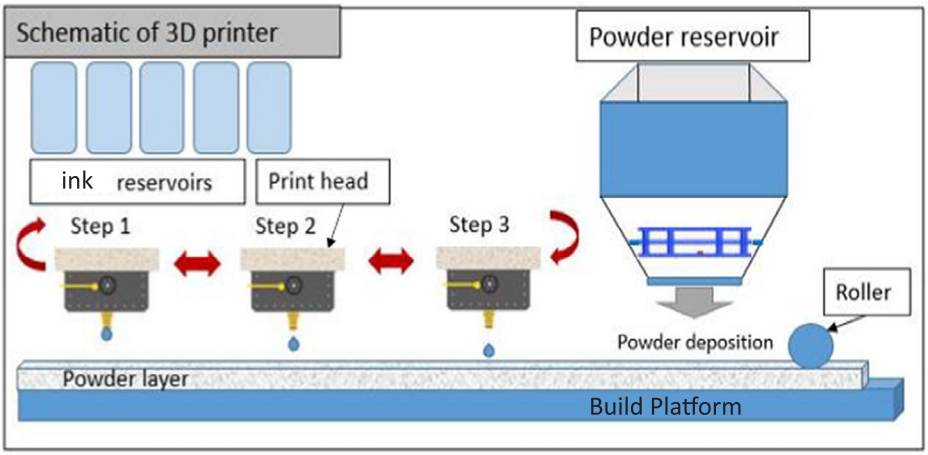

Fig. 1. Schematic of inkjet-based 3D printing machine and sequence of the printing processa. a. Deposition of powder from the hopper onto the build platform. b. Spreading of the powder mixture on the platform by the roller. c. Spraying of ink solution by the printheads on top of the spread powder layer.

calcium Phosphate Anhydrate at 45, 10 and 45% (w/w). A V-blender was used for mixing at 40% fill volume. The mixing regime of the blending process was verified by calculating a dimensionless number, such as Froude number, as previously verified by our group (SPRITAM, xxxx). The Froude number (F_r) of 0.2 is maintained during the studies, where $F_r = \Omega^2 R/g$, Ω is the rotation rate, R is the blender radius and is equivalent to $H/2$ (H = height of the blender), and g is the acceleration due to gravity. $F_r < 1$. This ensures that gravity forces are stronger than the centrifugal forces, while $F_r < 0.4$ ensures the mixing to be dominated by tumbling motion during V-blending. The reason for maintaining tumbling motion and Fr < 0.4 during V-blending is to reach an optimum degree of mixing for the excipient mixture.

Design of the 3D printed tablet- A 3D printing process requires a tablet image file be sent to the printer prior to the start of a printing process. The most common image format that is compatible with all printers is stereolithographic (.STL) format. Tablets can be designed using any commercial computer-aided design and drafting software application. The tablet image file for this study was designed using Autodesk® 3ds Max Design 2016 software version 18.0 (Autodesk, Inc., USA). Afterwards, the image file was converted to stereolithography (.STL) format using 3D printer software. Next, via the image file, tablets were printed using an excipient mixture and API ink in the 3D system's binder-jet-based printer ProJet CJP 660 Pro (3D systems, Inc. USA). The CPJ printer involves two major components: core material and a binder solution, based on the binder jetting technology developed by the Massachusetts Institute of Technology. First, the 3D printer spreads the core material in a thin layer so that the binder solution will help to bind the core material that is injected by the printheads. According to the manufacturer's specifications, this can be achieved at a layer thickness of 100 μm. The printer properties, such as resolution-high and the powder layer height- 100 μm, were adjusted in the printer software (3D Sprint) using the installed graphical user interface (GUI) settings.

Rheology Studies- A rotational rheometer ARG2 (TA Instruments, Elstree, Hertfordshire, UK) was used with cup and bob geometry with 1 mm instrumental distance in linear mode. The ink samples were measured using a logarithmic sweep and steady state sensing at a shear rate of 1–300 sec^{-1}. The system temperature was maintained at 25 °C (printing temperature). Three replications for each sample were carried out in different sample orders.

Surface tension measurement- A OCA50 DataPhysics drop contour analysis system was used to measure the surface tension of the API inks. The samples were measured using the pendant drop method with 10 μL drop in an electronic multiple direct dosing system DDE/x. The temperature of the system was maintained at 25 °C in an air-droplet interface. A total of five replications for each sample were performed in different sample orders.

Thermal Analysis- The samples (individual formulation excipients, excipient mixtures, API loaded excipient mixtures and printed tablets) were placed in standard aluminum pans (TA instruments, Elstree, Hertfordshire, UK) and were analyzed in differential scanning calorimetry (DSC) Q600 (TA Instruments, Elstree, Hertfordshire, UK). Modulated DSC was performed on samples of the individual components in the mixture. The Modulated DSC was performed with nitrogen as the purge gas using a heating rate of 2 °C/min at an amplitude of ± 0.50 °C within a period of 60 s from 40 °C to 215 °C. The average weight of the crimped samples were ~5 mg.

Thermogravimetric analysis was also performed on the excipient mixture using TGA Q500 (TA Instruments, Elstree, Hertfordshire, UK). Approximately 10–15 mg of sample was placed in sample holder and heated from 30 °C to 500 °C at a rate of 10 °C/min.

Stability test of the API ink solutions- The API ink (freshly prepared) was analyzed by stability testing at room temperature. Freshly prepared API ink was stored at 60% RH at 25 °C. Samples were collected at 0, 24 and 48 h and were subjected to HPLC to quantify the amount of the active ingredients.

X-ray diffractometer (XRD)- XRD analysis was carried out for the excipient mixture, API loaded excipient mixture and printed tablets, using a D2-Phaser X-ray diffractometer (Bruker, Germany). Scanning was performed from 2θ = 5° to 50° using a coupled twotheta/theta scan type with a 0.050 sec time step. The X-ray wavelength was 0.154 nm (Source Cu) at voltage of 30 kV.

Scanning Electron Microscopy (SEM)- The inkjet-based 3D printed tablets were analyzed using FEI Nova NanoSEM 450, a cold cathode field emission scanning electron microscope with the help of Thermo Noran System Six EDS and COMPASS Component Analysis.

Micro-CT Imaging- MicroCT measurement of the printed tablets was carried out using Scanco μCT40. The spatial resolution was maintained at μm scale.

Characterization of the printed tablets - For each batch, the compendial tests on the printed tablets were performed as per USP guidelines. The weight variation test was performed using a digital analytical balance (Mettler Toledo, USA) for 6 tablets. The mechanical tests of the printed tablets were carried out using a friability tester (Erweka, TA, Germany) where 10 tablets were randomly selected, weighed, and put in a friability tester for 4 min at 25 rpm. The 3D printed tablets were subjected to a Okey hardness tester (International INC. N.J, USA).A standard jaw plate and breaking force of 10 tablets was recorded by applying force on tablets at the rate of 3.5 mm/s.

Assaying of drug in the printed tablets by HPLC- Six (n = 6) tablets were randomly selected and weighed from each set and placed in a 100 mL volumetric flask. The volume of the flask was made up by adding water and sonicated for 3 h. The solution was later placed in a 2 mL auto-sampler vial. Afterwards, quantification was carried out in the HP series 1100 HPLC with C18 column (Phenomenex CA, USA). The mobile phase used in the method was Phosphate Buffer: Methanol (30:70) (Adjusted to pH 5 by adding 1 N Hydrochloric acid). The drug absorbance was recorded at 240 nm at ~5 min retention time. The injection volume used was 10 μL and the column temperature was set to 40 °C.

In vitro Drug release from the printed tablets- The *in vitro* release study for the tablets was carried out using modified USP II apparatus by Sotax (MA, USA). For the dissolution study, three (n = 3) (Gültekin et al., 2019) tablets from each batch were placed in the dissolution vessel containing 100 mL of 10 mM Phosphate buffer solution (pH 5). The paddle speed was set to 100 rpm and the system temperature was maintained at 37 °C. Samples (2 mL) were collected at 0, 10, 20, 30, 60, and 120 min using pipettors with 2 mL capacity. Afterwards, the samples were centrifuged in an Eppendorf (CT, USA) centrifuge 5810R and placed in 2 mL HPLC auto-sampler vials. The quantitative analysis of the tablets was performed using the above mentioned HPLC protocol. All dissolution experiments were carried out under sink condition for all tablets.

3. Results & discussion

The goal of this study was (1) to evaluate the drug loading efficiency of an inkjet-based 3D printing process, and (2) to perform a pre-formulation analysis for printed tablets. The drug loading efficiency of the 3D printing process was measured by quantifying the printability property of API inks. Whereas the preformulation analysis was performed by thermal study and compendial tests on the drug loaded powder mixture and printed tablet, as well as by a stability study of the API ink solution.

3.1. Printability of API inks

Printability/jettability property of an ink can be defined as the ability of an ink to produce similar volume of droplets on every occurrence. This property of ink governs the jetting reproducibility in printed batches or, in this case, the reproducibility of drug loading in printed tablets. The printability of an API ink is printhead specific. The printhead (Fig. 2) consists of a printhead chamber (to store the ink

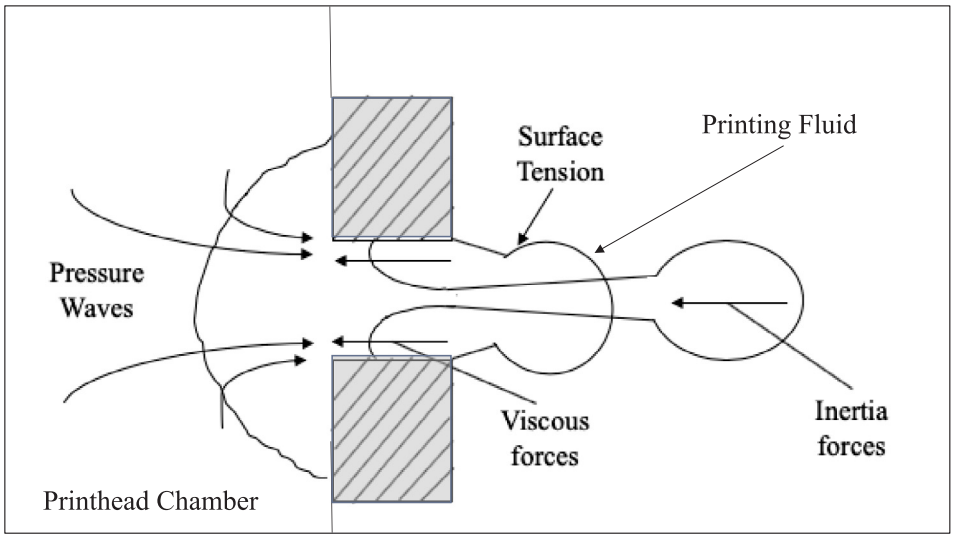

Fig. 2. Schematic of drop formation mechanism by the inkjet printhead during printing. a. Pressure Waves generated due to bubble information. b. Droplet formation of printing fluid governed by surface tension. c. Travelling of generated droplet due to interial force. c. Retreat of rest of liquid in the printhead due to the viscous force.

temporarily prior to jetting) and a nozzle plate (to jet out the ink)-consisting of several numbers of small nozzles. The jetting process of the API ink out of the printhead nozzle occurs by drop formation mechanism due to the pressure difference. A heater installed in the thermal printhead (specific for this study) generates a bubble that expands and propels a specific amount of ink through the printhead nozzles. As shown in Fig. 2, this propelled liquid is due to the surface tension and inertial forces that are created when it separates a droplet out of its volume. The droplets then travel down onto the powder bed due to gravity during printing. The rest of the lingering liquid inside the printhead returns to the printhead chamber via the nozzle. This happens due to bubble collapse inside the printhead chamber leading to a pressure drop and surface tension dominated liquid retreat. Therefore, the printability of the API ink is highly dependent on its surface tension, inertial force, and viscosity property (Guo et al., 2017; Derby, 2010; Speranza, 2019; Demaria, xxxx). This can be analyzed by an Ohnesorge number (*Oh*) (Eq. (1)); i.e. a dimensionless parameter representing all these properties together. *Oh* is a ratio of Reynold's (*Re*) and Weber's (We) number and can predict the jetting behavior of the ink solution; $Oh > 1$ dissipative viscous force dominates preventing drop ejection, whereas $Oh < 0.1$ produces uncontrolled satellite drops. The *Oh* number was calculated for every API ink in this study by measuring the viscosity, surface tension, and density of the ink solutions.

$$Oh = \frac{\sqrt{We}}{Re} = \frac{\mu}{\sqrt{\rho\gamma d}} = \frac{viscous\ \ force}{\sqrt{inertial.\ surface\ \ tension}} \quad (1)$$

ρ = *Density*

u = Velocity
d = Characteristic length
μ= Viscosity
γ= Surface tension *of the ink solution*

$$\text{We} = \frac{\rho u d}{\gamma} = \frac{inertial\ \ force}{surface\ \ tension\ \ force}$$

$$\text{Re} = \frac{\rho u d}{\mu} = \frac{inertial\ \ force}{viscous\ \ force}$$

Along with maintaining a printable *Oh* number to produce reproducible jetting, viscosity property of API inks was also maintained to incorporate printhead specific limitations. The printhead (dispenser of the ink) used in this study was a HP11 black printhead which has a jetting limitation (w.r.t viscosity to minimize nozzle wearing) standardized by HP for HP 11 black ink. Therefore, the viscosity of all the API ink prepared for the study was kept below the HP standard black ink solution.

To calculate the *Oh* number of the API inks, ink properties were measured with respect to viscosity, surface tension, and density. The viscosity of API inks was measured using an ARG2 cup and bob viscometer. The rheological profile of all API inks (of different drug loading) shown in Table 1 depicts that increasing drug loading increases the viscosity of the API inks.

The surface tension property of the inks was analyzed and quantified using pendant drop method.

The surface tension value of the standard solution used in the study (HP 11 black) was 30 N-m. Table 1 represents the surface tension of all API inks used in the study. Table 1 shows that surface tension of the API

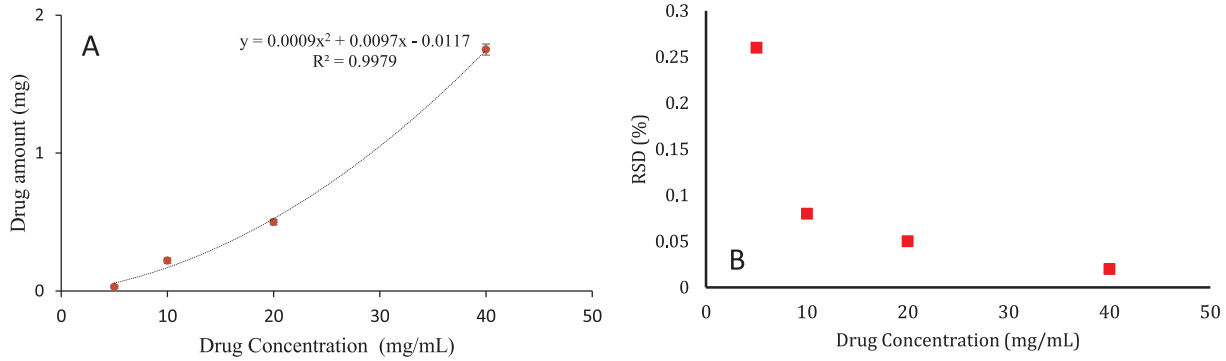

Fig. 3. (A) Content uniformity assay of 4 types of AMT loaded 3D printed tablets in UV-HPLC (n = 6). (B) RSD deviation of 4 types of AMT loaded 3D printed tablets (n = 6).

Table 1
Characterization of the ink solutions used in the study.

API Ink	Concentration (mg/mL)	Viscosity (kg/ms^2)	Surface Tension (kg/s^2)	Density (kg/m^3)	Characteristic Length (m)	Oh
1	40	0.00434	0.0520	0.98	1.8×10^{-5}	0.14
2	20	0.00395	0.0533	0.99	1.8×10^{-5}	0.13
3	10	0.00347	0.0560	0.99	1.8×10^{-5}	0.11
4	5	0.00332	0.0627	1.00	1.8×10^{-5}	0.10

ink decreases with increasing drug concentration. This indicates that the AMT has surface-active properties and, upon increasing the amount of the drug in the ink, the amount of the drug on the surface increases consequentially, thereby decreasing surface tension in the API ink. The importance of this observation suggests that surface tension property of an ink can be modulated by controlling the amount of API or other surface active agents that are added to it. This observation can be used as an alternative way to develop an ink solution for study by adjusting the surface tension of an ink to the surface tension value of a standard ink; i.e. HP 11 black ink to maintain the efficient jettability of the ink formulations.

The density of the ink solutions was quantified by weighing 1 mL of ink solution in a weighing apparatus and calculating the density by dividing the weight over volume of the ink solution.

By using viscosity, density, and surface tension data, the Oh number was calculated for all ink solutions (Table 1). The Oh number of ink solutions was well in between $0.1 < Oh < 0.14$, thereby providing stable printability of the API ink solutions.

The drug loading efficiency of the printing process was also quantified by performing a drug assay on the printed tablets acquired using four different concentration of Amitriptyline Hydrochloride (AMT) loaded in the API inks. To study the efficiency of drug loading in printed tablets through the jetting process, AMT was chosen for the study because of its thermal stability and inert nature. The drug loads on the printed tablets were 1.75 mg, 0.5 mg, 0.22 mg and 30 µg. The precision and accuracy of the drug loading was optimal, although a higher deviation was observed on lower drug loading (as shown in Fig. 5). Fig. 3 A represents the drug loading capacity of the printing process dependent on the drug loading of the ink solution. The non-linearity of the graph represents the effect of several factors, such as surface tension and viscosity of the printing fluid governing the amount of fluid reaching the printed tablets in the printing process. Further investigation of the cause was not carried as it was outside of the scope of this study. Fig. 3 B supports the accuracy of the printing process representing a relative standard deviation of < 0.3.

3.2. Preformulation analysis

To perform a pre-formulation analysis, the tablets and the drug loaded formulation mixture were evaluated based on physical characteristics, such as compendial tests of the printed tablets (weight variation, hardness, friability, and disintegration time), along with thermal studies of both the tablets and the formulation mixture using Differential scanning calorimetry (DSC) and Thermogravimetric analysis (TGA).

The 3D printed tablets were evaluated for weight variation test, hardness, dimensions, and friability (Table 2). The hardness of the printed tablets ranges from 3.6 −5.0 kg/cm^2 which is standard for conventional pharmaceutical tablet dosage form. The friability of the printed tablets was < 0.87%, thereby endorsing the successful implementation of immediate release tablet dosage form development protocol using a binder-jet 3D printing process. The disintegration time for the printed tablets was less than 2 min indicating the advantage of the binder-jet 3D printing process as compare to other printing processes, such as FDM, where the disintegration time of the fabricated tablets is at least ~5 min (Alomari et al., 2015). The *in vitro* release pattern of the printed tablets reveals the release kinetics of the printed tablets where more than 80% of the drug is released in the medium by 30 min.

Thermal analysis was performed on the powder mixture, AMT loaded powder mixture, and printed tablets. However, due to the low drug loading, it was not possible to detect the presence of the drug in the printed tablets by modulated DSC as shown in Figs. 4 and 5.

XRD could not reveal the presence of drug as drug loading was very low, but data could be used to study the drug excipient interaction (Fig. 6).

Thermogravimetric analysis of the individual powders, powder mixture, and AMT loaded powder mixture was performed to analyze the degradation profile of the samples. A full TGA profile of the AMT loaded physical mixture explains the possible thermal events occurring in the mixture due to the temperature increment. As shown in Fig. 7, temperatures of 30 to 80 °C show moisture loss from the AMT loaded physical mixture, whereas at 80–126 °C Lactose Monohydrate losses its bound water. On further temperature increments, the sample displays AMT, Lactose, and PVP K30 degradation at 190–250 °C, 250–330 °C, and 330–485 °C, respectively. As the degradation temperature of Di-

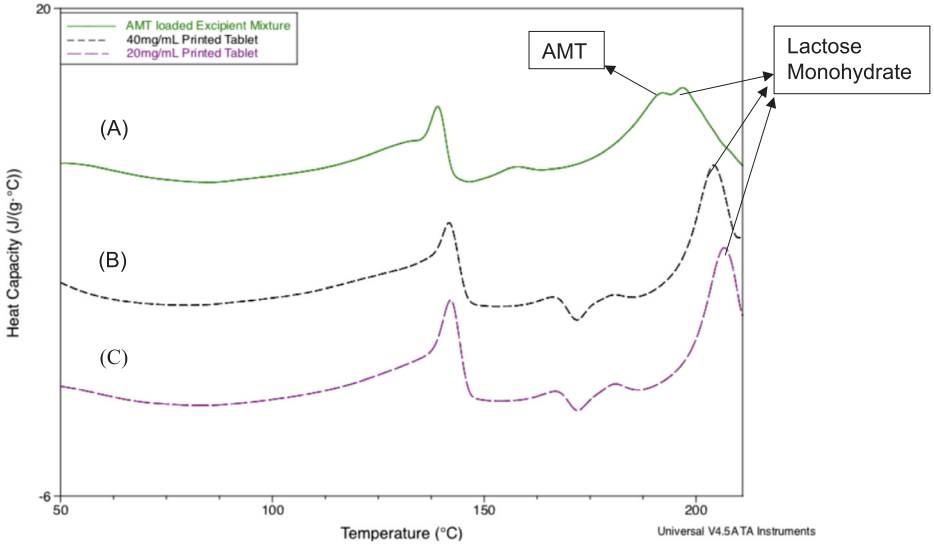

Fig. 4. DSC thermal analysis profile of API loaded. Excipient mixture (A), 40 mg/mL (B) and 20 mg/mL. (C) API containing print fluid loaded printed tablets.

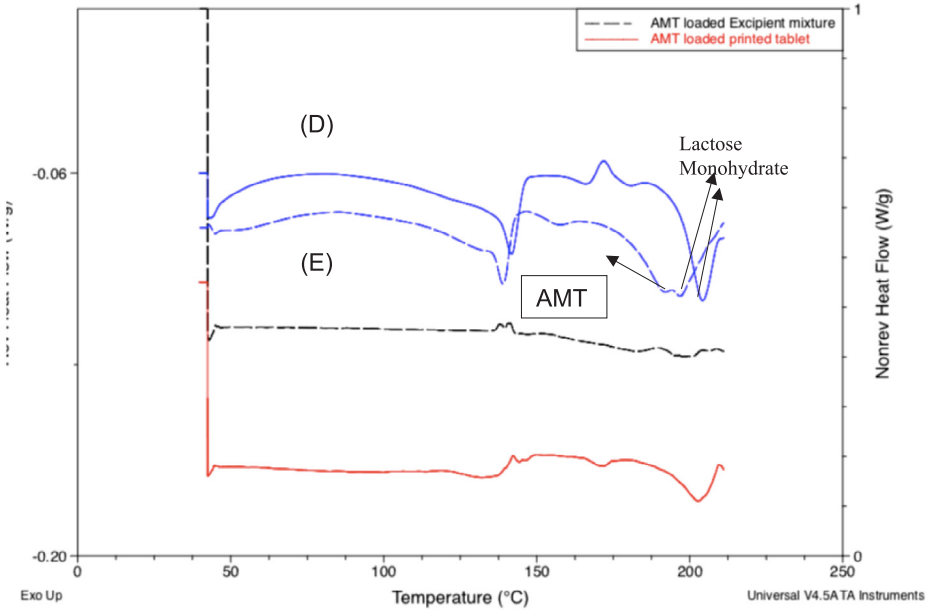

Fig. 5. Modulated DSC (MDSC) thermal analysis profile of 40 mg/mL (D) and 20 mg/mL (E) API containing print fluid loaded printed tablets to observe minute thermal changes due to the presence of drug but due to low drug loading the drug was undetectable in the printed tablets using MDSC.

Table 2
Characterization results of the printed batches recovered from the printing.

API ink (mg/mL)	Weight variation (gm)	Breaking force (kgf)	Friability (%)	Disintegration test (s)	Diameter (mm)	Height (mm)
5	218 ± 3.95%	3.67 ± 0.55	< 0.50	79.33 ± 3.54	8.3 ± 0.17	5.1 ± 0.15
10	244.3 ± 2.9%	4.87 ± 0.32	< 0.56	88.67 ± 1.15	8.4 ± 0.12	5.2 ± 0.1
20	230.4 ± 1.4%	4.93 ± 0.76	< 0.48	89 ± 4	8.4 ± 0.5	5.2 ± 0.12
40	230.5 ± 1.26%	5 ± 0.8	< 0.70	82 ± 4.2	8.3 ± 0.17	5.2 ± 0.17

Calcium phosphate anhydrate is around ~1500 °C, the TGA profile of the AMT loaded mixture did not display any degradation peak. The excipient mixture shows no significant weight loss in TGA within the 3D printing operating range (till 35 °C). Heating beyond 220 °C leads to two steps of degradation at approximately 280 °C and 410 °C (as shown in Figs. 8 and 9).

For the pre-formulation analysis, a compendial study of the printed tablets and stability study of API ink solution were also performed.

To assess the stability of the API ink from preparing an ink until the end of a printing cycle, API ink solutions were subjected to a stability study. The stability test results of the API ink solution indicated that there is no significant change in the concentration of amitriptyline hydrochloride from day 0 to day 2. This indicates that the ink solution is stable during the duration of preparation time until the end of a printing cycle at room temperature (as shown in Table 3). The thorough stability test was also carried out at the advent and end of a printing process to evaluate any drug degradation that may occur in the ink solution due to the temperature increment inside the printhead while printing (as shown in Table 3). This was accomplished by collecting the ink solution discarded in the waste tray of the printer during a printing cycle.

A CAD file of the designed tablet was developed using AutoCAD software and 3D print Pro software that was sent to the printer prior to printing. The tablet design parameters (5.3 (Height-H), 8.4 (Width-W)

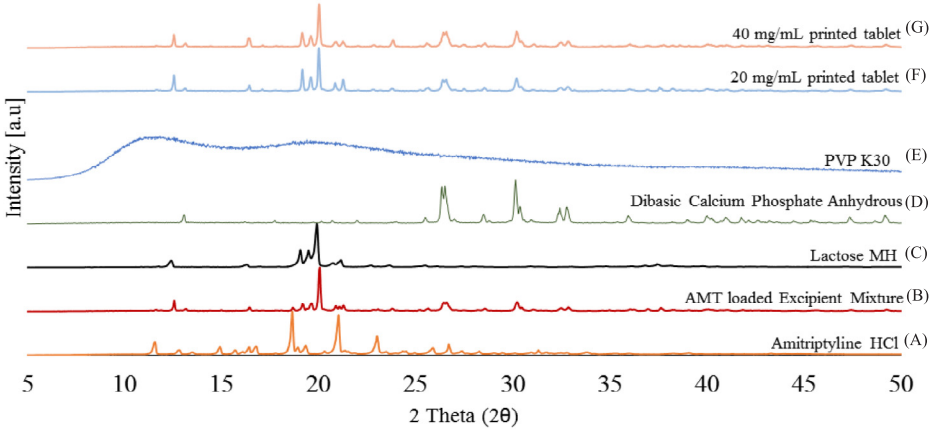

Fig. 6. XRD Patterns of the API (AMT)(A), individual excipients (C-E), API loaded excipient mixtures (B) along with 40 mg/mL (F) and 20 mg/mL (G) API containing print fluid loaded printed tablets.

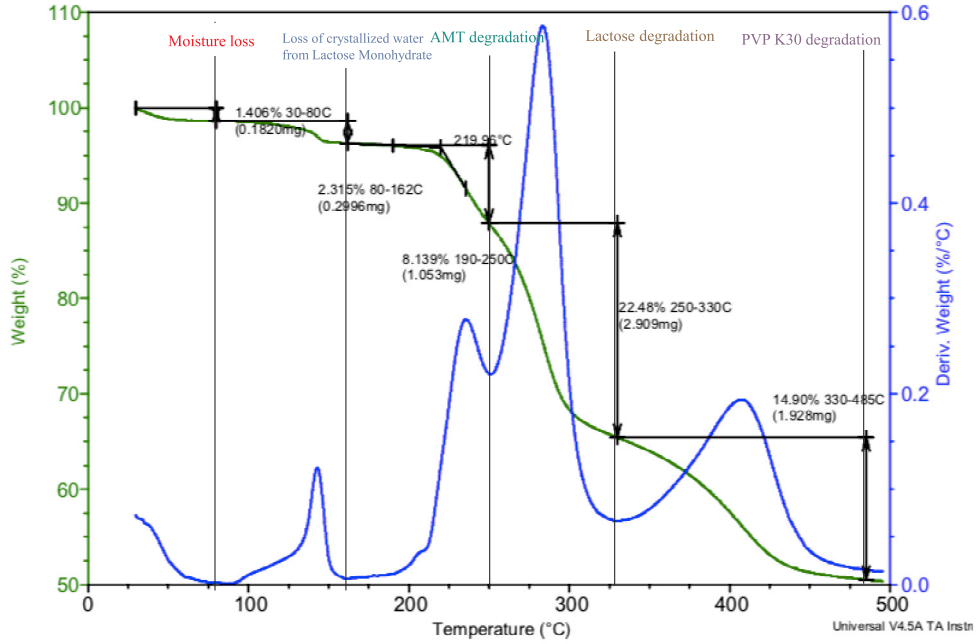

Fig. 7. TGA thermal degradation profile of AMT loaded formulation mixture exhibiting distinct degradation of individual excipient including API (AMT).

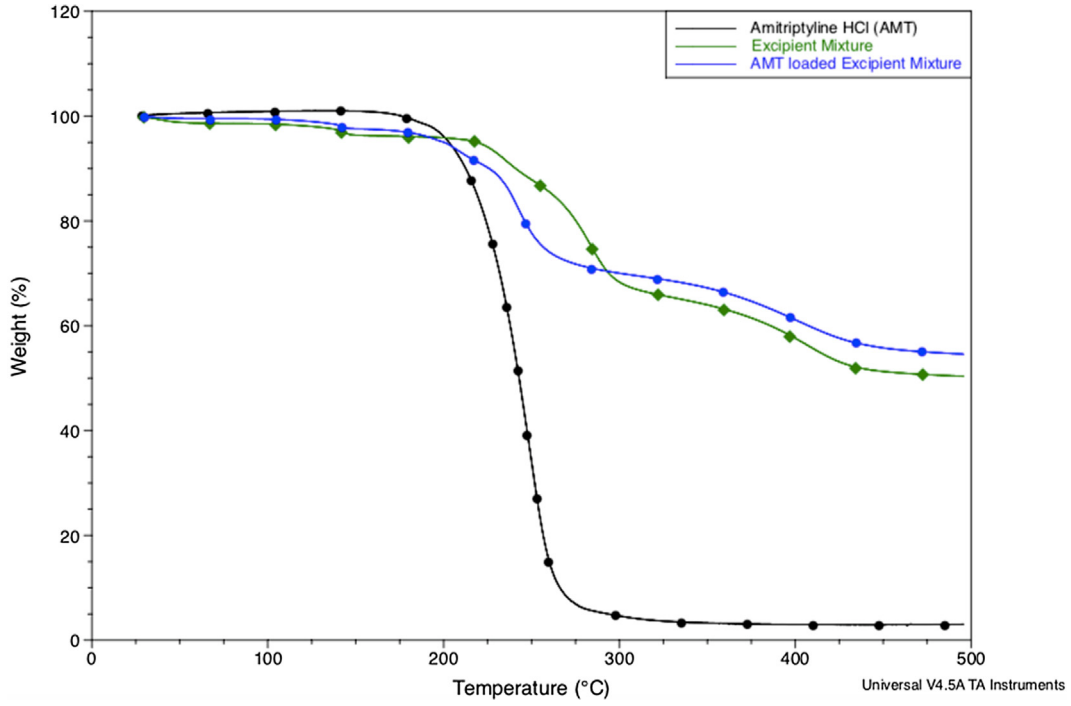

Fig. 8. TGA thermal degradation profile of API (Amitriptyline Hydrochloride/AMT), Excipient/powder mixture, and AMT loaded formulation mixture.

and 8.4 (Diameter-D) mm) were kept constant throughout all the printing (as shown in Fig. 10). To understand the drug release profile from the tablets with different concentration of the drug (inks), same dimension (8.4 (W) × 5.4 (H)) tablets were printed (as shown in Fig. 11) and different drug loading (1.75, 0.5, 0.22 mg and 30 μg) were achieved.

To characterize the printed tablets, an HPLC protocol was developed and *in vitro* release patterns of the printed tablets were studied. A calibration curve was developed with different AMT concentrations, from 2.5 μg/mL to 20 μg/mL, by dissolving the AMT drug in a medium containing all the other formulation excipients. Three replications of each data point were carried out while considering intra and inter-day variation. The calibration curve had correlation of R^2 = 0.995. The study was carried out with Phenomenax C18 column (particle size: 5 μm) with a flow rate of 1 mL/min and injection volume of 10 μL at 40 °C, pH 5. 10 mN was used as the medium and the retention time of the drug was recorded at 4.7 min.

The *in vitro* release pattern of Amitriptyline Hydrochloride (AMT) from the printed tablets was studied in a modified USP 2 apparatus dissolution system for a period of 2 h. Due to the observation during dissolution, it was apparent that the printed tablets were entirely disintegrated at almost 1.5 min into the dissolution test. The highly water-soluble drug, i.e. AMT, was released from the disintegrated portion of the tablets and dissolved in the dissolution medium. Immediate release

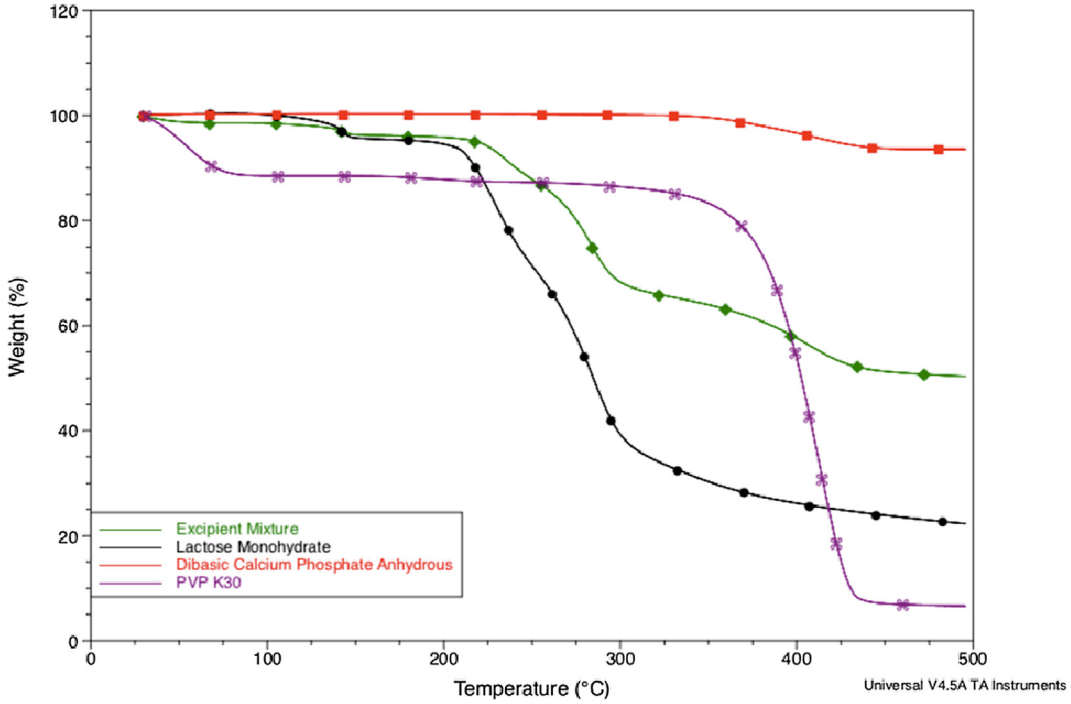

Fig. 9. TGA thermal degradation profile of excipient mixture, and individual components of the excipient mixture i.e. Lactose Monohydrate, Dibasic Calcium Phosphate Anhydrous and PVP K30.

Table 3
Stability test of the freshly prepared API ink solutions (n = 3).

API ink (mg/mL)	Content (%)		
	0 h	24 h	48 h
40	100.7 ± 2.42	101.42 ± 2.5	100.4 ± 1.09
20	100.3 ± 3.60	99.11 ± 1.15	98.59 ± 2.43
10	99.4 ± 2.09	99.55 ± 3.25	98.90 ± 2.9
5	99.5 ± 1.35	99.85 ± 1.5	99.79 ± 3.8

Fig. 10. Photographs of 3D printed tablets.

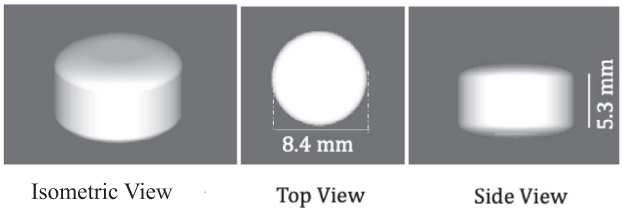

Fig. 11. CAD designed image file used in the printing process.

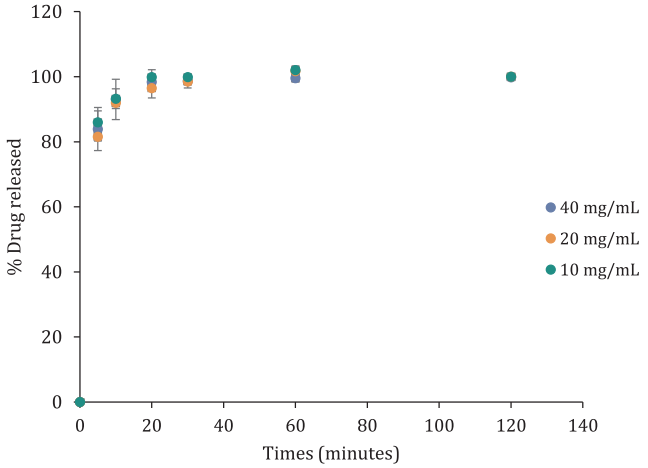

Fig. 12. *In-vitro* dissolution profile of the printed tablet batches (n = 3), exhibiting as immediate release property of the printed tablets by releasing > 90% of the drug in 30 min.

properties were observed in the printed tablets, i.e. > 85% of the drug was released in first 30 min (as shown in Fig. 12).

SEM and micro-CT imaging was conducted to study the physical characteristics of the printed tablets. The SEM image of the AMT loaded printed tablets shows the rough surface structure of printed tablets in Fig. 13. Whereas the EDS (chlorine [Cl^-] mapping) of the same sample (Fig. 14(a) and (b)) qualitatively represents (the blue dots) the distribution of the drug Amitriptyline HCl over the sample surface. The cross-sectional area of the printed tablets also displays equal distribution of AMT, thereby confirming the presence of the drug in every layer of the printed tablet.

SEM and Micro-CT imaging of the printed tablets clearly show the external rough structure of the tablets with noticeable porous gaps or voids on the surface (Fig. 15) providing a reasonable explanation of quick disintegration of the printed samples.

A comprehensive study was performed by producing drug loaded

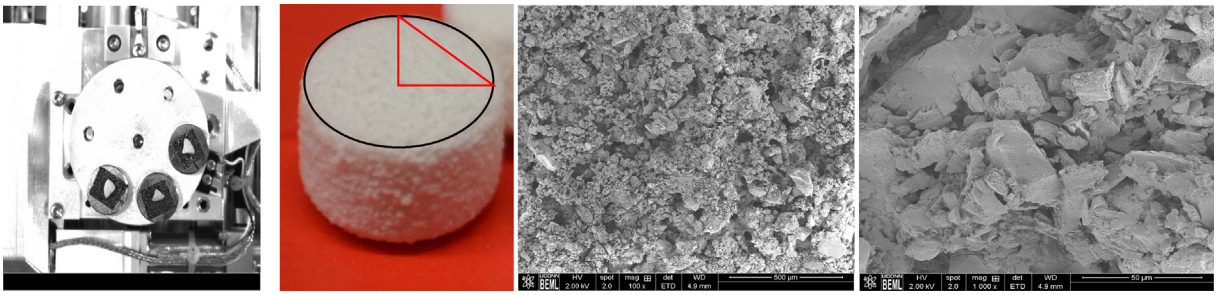

Fig. 13. SEM picture of the printed tablet to view the surface of the 3D printed tablet.

binder-jet 3D printed tablets to evaluate the drug loading efficiency of the printing process and physical properties of the printed tablets. A common tablet design file was prepared and used for all the printing batches. The critical material attributes of the feedstock/ raw materials, such as the ink solution and the excipient mixture, were characterized to maintain reproducibility of the printing process and to study the stability of the dosage printlets. Ink solution and excipient mixture were loaded onto the printer, whereas a tablet design file was loaded in the printing software prior to every printing cycle. According to Fig. 16, the API ink solution was formulated by mixing the drug in deionized- distilled water (with resistance of 18.2Mohm) at 60 rpm for 12 h followed by sonication for 2 h at room temperature. Likewise, the excipient mixture was prepared by mixing in a V-blender at 40% fill for 18 min at 29 rpm. The feed materials of the printer, such as the API ink and the excipient mixture, were then loaded onto the ink reservoir and the powder reservoirs installed in the printer, respectively, prior to the printing process.

The compendial tests of the printed tablets show the physical properties of the printed samples, such as weight, shape (dimensions), hardness, friability, and disintegration, providing the critical quality attributes of the printed product samples. The micro-CT and the SEM images of the printlets clearly show the patterns of layer by layer deposition of the excipient mixture and the porous structure of the printed tablets, respectively. This is unlike conventionally manufactured tablets and explains the quick disintegration time of the printlets upon coming in contact with water. The assay result and the RSD (variation) graph show the drug loading efficiency onto the printed tablets corroborating optimized precision of the printing process. The dissolution data provides an inside of the drug release kinetics of the printed samples.

4. Conclusions

The drug loading efficiency of the binder-jet 3D printing process was evaluated by loading Amitriptyline Hydrochloride (API) in the ink formulation. The API was loaded effectively in ink, and the drug loading of the printed tablets was achieved in the microgram scale with higher precision, which is a novel step in the tablet manufacturing field. The pre-formulation analysis of the drug-loaded physical mixture and the printed tablets was performed by thermal analysis and compendial tests, respectively. The compendial characterization of the printed tablets was evaluated with respect to weight variation, hardness, disintegration, and size, and the resulting data are as shown in Table 2. The stability of the API ink solution was assured by performing an assay test of the jetted ink collected in the waste tray during the printing process. The SEM-EDS mapping of the printed tablet has given an idea of the distribution of the drug qualitatively, whereas UV-HPLC corroborated the presence of AMT in the printed tablets quantitatively. The micro-CT images of the printed tablets show the porous surface structure, and the *in vitro* release test of the printed tablets aid in understanding that the fabricated tablets have immediate release properties.

To the author's knowledge, this is the first report of the loading of API in ink to increase the content uniformity of printed tablets by using the precision and accuracy of the powder-based binder-jet 3D printing process. Furthermore, this is the first documented reporting of such low drug loading using a binder-jet 3D printing process in pharmaceutical tablet fabrication.

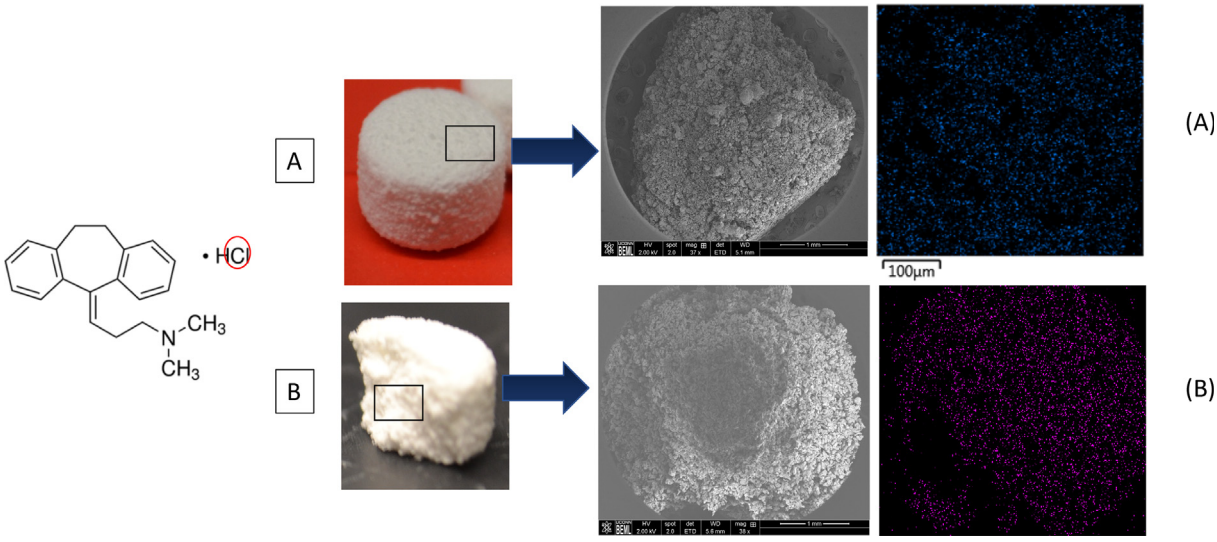

Fig. 14. EDS spectrum, and element mapping images for Cl- ions of the surface and cross section of the 3D printed tablets. The blue and pink dots indicates the presence of Cl- ions on the surface and throughout the cross of the tablets confirming the distribution of the API (AMT). (For interpretation of the references to color in this figure legend, the reader is referred to the web version of this article.)

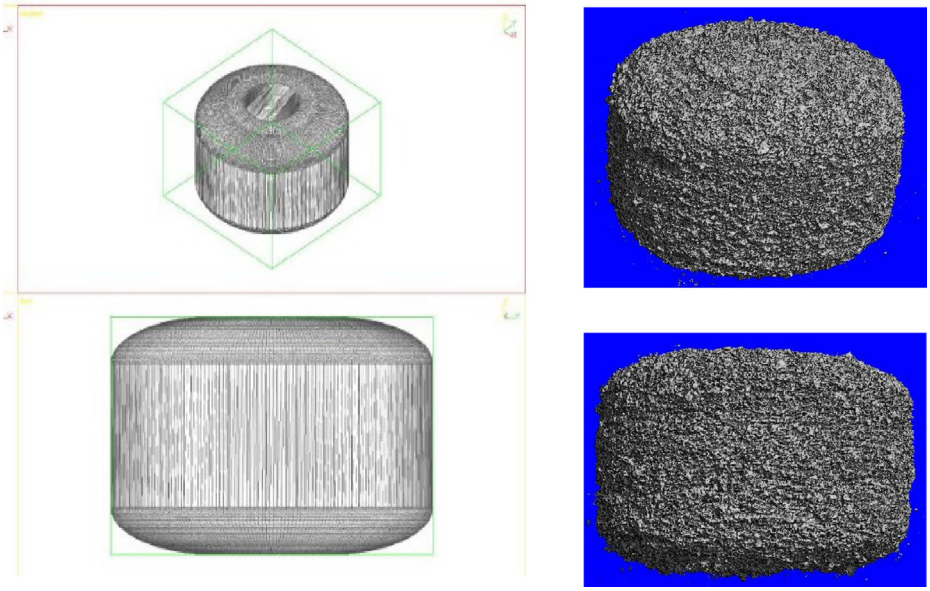

Fig. 15. Micro-CT images of AMT loaded 3D printed tablets exhibiting a porous structure of the printed tablets.

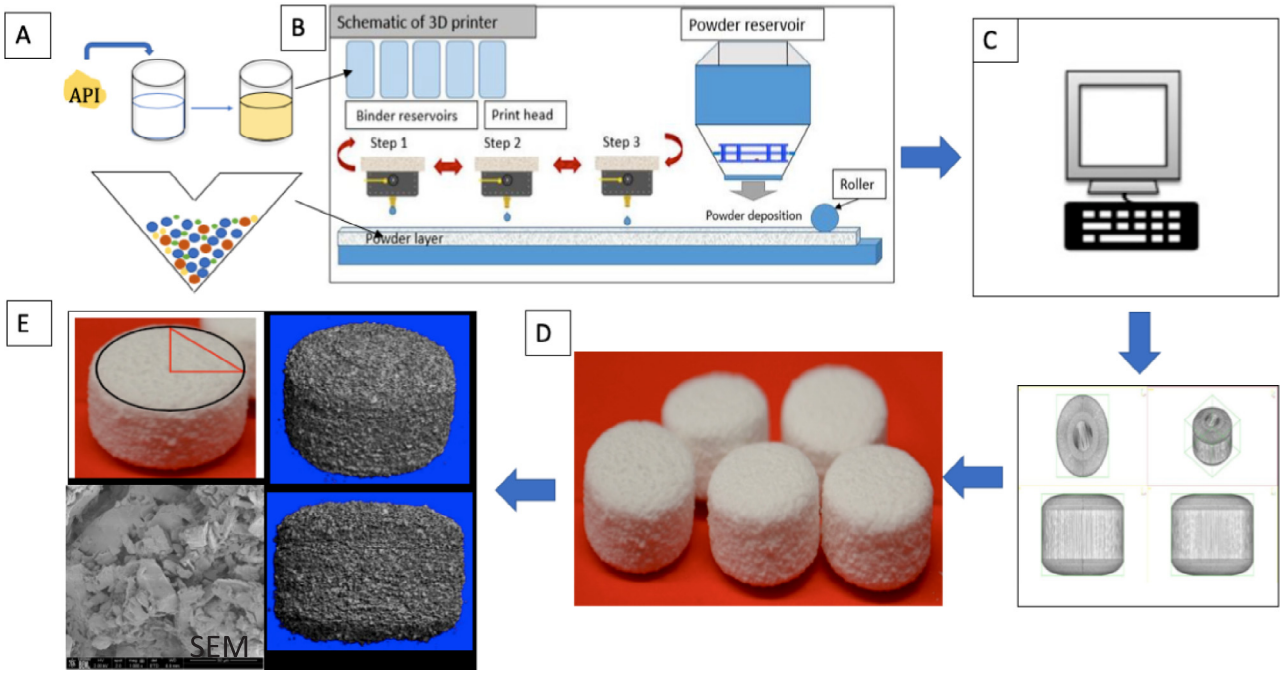

Fig. 16. Schematic illustration of immediate release tablet fabrication using inkjet-based 3D printing process. a. API ink was prepared by mixing the API i.e. AMT in the water followed by sonication and the powder mixture is prepared by mixing the excipient in a V-blender b. Both API ink and the powder mixture are loaded onto the 3D printer as feed materials c. Tablet CAD designed file were developed prior to the printing process and sent to the printer d. Immediate release tablet dosage forms are fabricated using inkjet based 3D printing process e. SEM and Micro-CT images were obtained to understand the surface properties and the external structure of the 3D printed tablets.

CRediT authorship contribution statement

Koyel Sen: Conceptualization, Methodology, Formal analysis, Writing - original draft, Writing - review & editing, Visualization. **Arushi Manchanda:** Conceptualization, Methodology, Formal analysis, Writing - review & editing. **Tanu Mehta:** Formal analysis. **Anson W.K. Ma:** . **Bodhisattwa Chaudhuri:** Conceptualization, Methodology, Writing - review & editing.

Declaration of Competing Interest

The authors declare that they have no known competing financial interests or personal relationships that could have appeared to influence the work reported in this paper.

Acknowledgements

We are grateful to the Center for Pharmaceutical Processing Research (CPPR) for providing funds for this research. We want to thank Aastrazeneca (AZ), Boehringer Ingelheim (BI), Abbvie, and

Genentech for mentorship.

References

Khaled, S.A., Burley, J.C., Alexander, M.R., Roberts, C.J., 2014. Desktop 3D printing of controlled release pharmaceutical bilayer tablets. Int. J. Pharm. https://doi.org/10.1016/j.ijpharm.2013.11.021.

Rowe, C.W., Katstra, W.E., Palazzolo, R.D., Giritlioglu, B., Teung, P., Cima, M.J., 2000. Multimechanism oral dosage forms fabricated by three dimensional printing(TM). J. Control. Release. https://doi.org/10.1016/S0168-3659(99)00224-2.

Sandler, N., Määttänen, A., Ihalainen, P., Kronberg, L., Meierjohann, A., Viitala, T., Peltonen, J., 2011. Inkjet printing of drug substances and use of porous substrates-towards individualized dosing. J. Pharm. Sci. https://doi.org/10.1002/jps.22526.

Sastry, S.V., Nyshadham, J.R., Fix, J.A., 2000. Recent technological advances in oral drug delivery - A review. Pharm. Sci. Technol. Today. https://doi.org/10.1016/S1461-5347(00)00247-9.

Jivraj, M., Martini, L.G., Thomson, C.M., 2000. An overview of the different excipients useful for the direct compression of tablets. Pharm. Sci. Technol. Today. https://doi.org/10.1016/S1461-5347(99)00237-0.

Unit Processes in Pharmacy: Operations. 2013. Encyclopedia Pharm. Technol., 457–485 doi:10.1201/b19309-34.

Scoutaris, N., Alexander, M.R., Gellert, P.R., Roberts, C.J., 2011. Inkjet printing as a novel medicine formulation technique. J. Control. Release. https://doi.org/10.1016/j.jconrel.2011.07.033.

Skowyra, J., Pietrzak, K., Alhnan, M.A., 2015. Fabrication of extended-release patient-tailored prednisolone tablets via fused deposition modelling (FDM) 3D printing. Eur. J. Pharm. Sci. https://doi.org/10.1016/j.ejps.2014.11.009.

Tutton, R., 2012. Personalizing medicine: Futures present and past. Soc. Sci. Med. https://doi.org/10.1016/j.socscimed.2012.07.031.

Stability of Drugs and Dosage Forms, 2002. Stability of drugs and dosage forms. https://doi.org/10.1007/b11444.

Wang, J., Goyanes, A., Gaisford, S., Basit, A.W., 2016. Stereolithographic (SLA) 3D printing of oral modified-release dosage forms. Int. J. Pharm. https://doi.org/10.1016/j.ijpharm.2016.03.016.

Okwuosa, T.C., Stefaniak, D., Arafat, B., Isreb, A., Wan, K.W., Alhnan, M.A., 2016. A lower temperature FDM 3D printing for the manufacture of patient-specific immediate release tablets. Pharm. Res. https://doi.org/10.1007/s11095-016-1995-0.

SPRITAM (Levetiracetam) Tablets. Accessdata.fda.gov, www.accessdata.fda.gov/drugsatfda_docs/nda/2015/207958Orig1s000TOC.cfm.

Genina, N., Janßen, E.M., Breitenbach, A., Breitkreutz, J., Sandler, N., 2013. Evaluation of different substrates for inkjet printing of rasagiline mesylate. Eur. J. Pharm. Biopharm. https://doi.org/10.1016/j.ejpb.2013.03.017.

Gala, R.P., Morales, J.O., McConville, J.T., 2019. Preface to advances in thin film technologies in drug delivery. Int. J. Pharm. https://doi.org/10.1016/j.ijpharm.2019.118687.

Alomari, M., Mohamed, F.H., Basit, A.W., Gaisford, S., 2015. Personalised dosing: printing a dose of one's own medicine. Int. J. Pharm. https://doi.org/10.1016/j.ijpharm.2014.12.006.

Guo, Y., Patanwala, H.S., Bognet, B., Ma, A.W.K., 2017. Inkjet and inkjet-based 3D printing: connecting fluid properties and printing performance. Rapid Prototyp. J. https://doi.org/10.1108/RPJ-05-2016-0076.

Mukherjee, R., Gupta, V., Naik, S., Sarkar, S., Sharma, V., Peri, P., Chaudhuri, B., 2016. Effects of particle size on the triboelectrification phenomenon in pharmaceutical excipients: experiments and multi-scale modeling. Asian J. Pharm. Sci. https://doi.org/10.1016/j.ajps.2016.04.006.

Gültekin, H.E., Tort, S., Acartürk, F., 2019. An effective technology for the development of immediate release solid dosage forms containing low-dose drug: fused deposition modeling 3D printing. Pharm. Res. https://doi.org/10.1007/s11095-019-2655-y.

Derby, B., 2010. Inkjet printing of functional and structural materials: fluid property requirements, feature stability, and resolution. Annu. Rev. Mater. Res. https://doi.org/10.1146/annurev-matsci-070909-104502.

Speranza, R., 2019. Nanophotonic approaches to colourful solar cells and modules. Politecnico di Torino.

Demaria, C. https://www.centropiaggio.unipi.it/sites/default/files/course/material/2017-11-08_-_inkjet_printing_part_2.pdf.